Wnt10b signaling regulates replication stress-induced chromosomal instability in human cancer

Alexander Haas[1], Friederike Wenz[1], Janine Wesslowski[3], Gary Davidson[3], Oksana Voloshanenko[3], Michael Boutros[3], Sergio Acebron[4] and Holger Bastians[1,*]

[1] University Medical Center Göttingen (UMG), Department of Molecular Oncology, Section for Cellular Oncology, Göttingen Center for Molecular Biosciences (GZMB), 37077 Göttingen, Germany. [2] Karlsruhe Institute of Technology (KIT), Institute of Biological and Chemical Systems-Functional Molecular Systems (IBCS-FMS), 76344 Eggenstein-Leopoldshafen, Germany. [3]Division of Signaling and Functional Genomics, German Cancer Research Center (DKFZ) and Department of Molecular Human Genetics, Institute of Human Genetics, Medical Faculty Heidelberg, Heidelberg, Germany [4] Heidelberg University, Centre for Organismal Studies (COS), 69120 Heidelberg.

* corresponding author: Holger Bastians, Email: holger.bastians@uni-goettingen.de

Running title: Wnt signaling and genome instability

Keywords: aneuploidy, chromosomal instability, mitosis, replication stress, Wnt10b.

Summary blurb

We describe a novel role of Wnt10b signaling acting in response to DNA replication stress to suppress chromosomal breaks and mitotic errors in human cancer cells.

Abstract

Wnt signaling pathways are involved in various developmental and tissue maintenance functions while deregulated Wnt signaling is closely linked to human cancer. Recent work revealed that loss of Wnt signaling impairs mitosis and causes abnormal microtubule growth at the mitotic spindle resulting in chromosome missegregation and aneuploidy, both of which are hallmarks of cancer cells exhibiting chromosomal instability (CIN). Here, we demonstrate that Wnt signaling specifically activated by Wnt10b is relevant in colorectal cancer cells to prevent abnormal microtubule dynamics and chromosome missegregation. Although mitosis is affected, Wnt10b signaling is required during the S phase of the cell cycle. In fact, Wnt10b signaling acts upon DNA replication stress in S phase, a condition typically associated with CIN in cancer, to prevent increased microtubule dynamics from S phase until mitosis, where they otherwise manifest in chromosome missegregation. Interestingly, replication stress-induced chromosomal breaks are also efficiently suppressed by Wnt10b. Thus, our results show that Wnt10b signaling regulates replication stress-induced chromosome missegregation and breakage, and hence, is a determinant for broad genome instability in cancer cells.

Introduction

Wnt signaling pathways play central and diverse roles in development and tissue homeostasis (Albrecht et al, 2021, Nusse et al, 2017). The best investigated example is the Wnt-β-catenin pathway that can be activated for instance by Wnt3a ligand leading to stabilization and activation of the transcriptional regulator β-catenin. This, in turn, drives the expression of a multitude of target genes contributing to the various cellular functions of Wnt signaling (Albrecht et al, 2021, Cadigan et al, 2012). Importantly, Wnt-β-catenin signaling is frequently upregulated in human cancer, particularly in colorectal cancer, where mutations in adenomatous polyposis coli (APC) cause hyper-stabilization of β-catenin (Schneikert et al, 2007, Zhan et al, 2017). Consequently, Wnt target genes including genes regulating the cell cycle are aberrantly expressed, thereby contributing to tumorigenesis and tumor progression (He et al, 1998, Tetsu et al, 1999). Wnt signaling can also stabilize proteins other than β-catenin. This is referred to as the "Wnt Stabilization Of Proteins (Wnt/STOP)" pathway, which was shown to be involved in the regulation of cell size and mitosis (Acebron et al, 2014, Hinze et al, 2019, Huang et al, 2015, Stolz et al, 2015b, Taelman et al, 2010). In fact, inhibition of β-catenin-independent Wnt signaling causes chromosome missegregation in mitosis leading to aneuploidy in human somatic cells as well as in pluripotent stem cells (Augustin et al, 2017, Jaime-Soguero d et al, 2024, Lin et al, 2021, Stolz et al, 2015b).

Perpetual mitotic chromosome missegregation promotes the evolvement of aneuploidy, which represent the basis for whole chromosome instability (W-CIN), a major form of genome instability and a hallmark of human cancer (Bakhoum et al, 2017, Chen X et al, 2024, Hanahan D & Weinberg RA, 2011, Lukow et al, 2022, Sansregret et al, 2018). W-CIN originates during mitosis and can be driven by various abnormalities leading to chromosome missegregation (Bastians & H., 2015, Devillers et al, 2024). Specifically, an abnormal increase in growth rates of microtubules within the mitotic spindle, which impairs the proper positioning of the spindle has been recently identified as an important mechanism leading to W-CIN in human cancer cells (Ertych et al, 2014, Ertych et al, 2016,

70 Paim et al, 2024, Schmidt et al, 2021, Tamura et al, 2020). In fact, chromosomally unstable cancer
71 cells that are characterized by high levels of chromosome missegregation typically display increased
72 spindle microtubule growth rates as a driver for aneuploidy, and thus, for W-CIN (Bohly et al, 2022,
73 Ertych et al, 2014, Tamura et al, 2020).

74 In contrast to W-CIN, structural CIN (S-CIN) causes structural chromosome aberrations including
75 DNA amplifications, deletions and translocations (Siri et al, 2021). S-CIN is often associated with
76 chromosomal breaks that are driven by defects in DNA repair or by slowed or stalled DNA replication,
77 a condition known as DNA replication stress (Siri et al, 2021, Zeman et al, 2014). Overall, CIN
78 represents a major form of genome instability and is a hallmark of human cancer (Hanahan D &
79 Weinberg RA, 2011, Sansregret et al, 2018). Consequently, CIN promotes tumor evolution by
80 generating genomic heterogeneity in cancer cells, thereby supporting aggressive growth
81 phenotypes, metastasis and therapy resistance (Bakhoum et al, 2017, Chen X et al, 2024, Lukow et
82 al, 2022, Sansregret et al, 2018).

83 Interestingly, S-CIN and W-CIN are typically detected concomitantly in chromosomally unstable
84 cancer cells suggesting functional links between the two forms of CIN (Burrell RA et al, 2013,
85 Janssen et al, 2011, Tijhuis et al, 2019). Indeed, several studies showed that replication stress can
86 not only trigger S-CIN, but also affects mitosis leading to chromosome missegregation and this can
87 be mediated by increase microtubule dynamics (Bohly et al, 2019, Bohly et al, 2022, Burrell RA et
88 al, 2013, Dwivedi et al, 2023, Wilhelm et al, 2019). In addition, we recently reported that, in
89 pluripotent stem cells, loss of Wnt can impact on DNA replication and, thereby supporting the
90 generation of mitotic errors (Jaime-Soguero d et al, 2024). However, it remains unclear what
91 mechanisms and pathways contribute to abnormal microtubule dynamics as a trigger for
92 chromosome missegregation in response to replication stress. Here, we show that in human cancer
93 cells Wnt10b signaling is required upon replication stress to ensure normal microtubule dynamics
94 from S phase until mitosis and to prevent chromosomal breaks and mitotic errors without affecting

95 DNA replication dynamics *per se*. Hence, we propose that Wnt10b signaling acts in cancer cells
96 during S phase-associated replication stress as a rescue pathway to limit genome instability.

97

98 **Results**

99

100 ***Loss of Wnt10b signaling causes mitotic errors.***

101 We have previously shown that loss of Wnt10b signaling causes mitotic errors in human somatic
102 cells (Fig. 1A). Of note, inhibition of Wnt(10b) signaling in chromosomally stable colorectal cancer
103 cells (HCT116), either at the canonical (co)receptor level by DKK1 treatment, by knockout of the Wnt
104 secretion factor *EVI/WNTLESS* (Augustin et al, 2017) or of *WNT10B* ligand (Fig. S1A) triggered
105 increased microtubule growth rates in mitotic cells as determined by live cell microscopy tracking of
106 individual microtubule plus tips within mitotic spindles (Fig. 1B,C). Increased mitotic microtubule
107 growth rates, in turn, were associated with increased chromosome missegregation during mitosis as
108 detected by the enhanced occurance of lagging chromosomes during anaphase of mitosis (Fig.
109 1D,E). The causal relationship between increased microtubule growth rates and chromosome
110 missegregation was validated by direct suppression of chromosome missegregation after restoration
111 of proper microtubule growth rates using sub-nanomolar concentrations of the microtubule-binding
112 drug Taxol as shown in previous studies (Fig. 1C,E)(Ertych et al, 2014, Stolz et al, 2015b). In all
113 conditions of suppressed Wnt signaling the mitotic errors were suppressed upon GSK3β kinase
114 inhibition indicating that Wnt-GSK3β signaling is involved in mitotic regulation (Fig. 1C,E)(Jaime-
115 Soguero d et al, 2024, Lin et al, 2021). Importantly, only treatment with purified Wnt10b, but not with
116 Wnt3a protein, rescued both, abnormally increased mitotic microtubule growth rates and
117 chromosome missegregation in HCT116-*WNT10B* and HCT116-*EVI/WNTLESS* knock-out cells,
118 even though Wnt3a was much more potent to activate Wnt/β-catenin signaling (Fig. 1C,E, Fig. S1B)

119 supporting the notion that β-catenin independent Wnt10b signaling is required for faithful
120 chromosome segregation (Lin et al, 2021, Stolz et al, 2015b).

121

122 ***Wnt10b signaling is required during S phase to ensure faithful mitotic chromosome***
123 ***segregation***

124 Since Wnt10b signaling is required for proper mitosis we expected it to act immediately before or
125 during mitosis to ensure normal mitotic microtubule dynamics and faithful chromosome segregation.
126 To test this, we treated cell cycle-synchronized HCT116 cells with DKK1 to induce mitotic errors or
127 synchronized HCT116-*EVI/WNTLESS* knock-out cells with purified Wnt10b to rescue mitotic errors
128 at specified phases of the cell cycle (Fig. 2A, Fig. S2). Surprisingly, DKK1-mediated inhibition of Wnt
129 signaling for only two hours during S phase, but not during G2 phase or immediately before or during
130 mitosis (G2/M) induced GSK3β-dependent abnormal microtubule growth rates and chromosome
131 missegregation (Fig. 2B, 2C). *Vice versa*, treatment of HCT116-*EVI/WNTLESS* knockout cells with
132 purified Wnt10b ligand rescued mitotic errors only when applied for two hours during S phase, but
133 not during later stages of the cell cycle, whereas treatment with Wnt3a from S phase until mitosis
134 had no effect (Fig. 2D,E). Thus, Wnt10b signaling seems to be required specifically during S phase
135 to ensure faithful chromosome segregation during the subsequent mitosis. To extend these findings
136 we used chromosomally unstable (CIN+) colorectal cancer cells, which are characterized by
137 inherently high rates of chromosome missegregation that are caused by increased microtubule
138 growth rates (Bohly et al, 2022, Ertych et al, 2014, Tamura et al, 2020). Also, in these CIN+ cancer
139 cells treatment with Wnt10b, but not Wnt3a specifically during S phase efficiently rescued abnormal
140 microtubule growth rates and chromosome missegregation in mitosis (Fig. 2F,G) indicating that
141 Wnt10b signaling is important during S phase to suppress mitotic errors in human cancer cells.

142

143 ***Inhibition of Wnt signaling increases microtubule growth rates from S phase into mitosis***

144 Since Wnt10b signaling is required during S phase but regulates mitosis several hours later we
145 wondered whether inhibition of Wnt signaling impacts microtubule behavior already before cells
146 enter mitosis. Thus, we determined interphase microtubule growth rates in synchronized cells with
147 or without Wnt inhibition (Fig. 3A). Interestingly, DKK1 treatment or loss of *EVI/WNTLESS* resulted
148 in increased microtubule growth rates in S phase and this abnormality was maintained until mitosis
149 (Fig. 3B). The same findings were obtained using synchronized CIN+ SW480 and SW620 cells that
150 exhibited inherently high microtubule polymerization rates from S phase until mitosis (Fig. 3C).
151 Importantly, treatment of synchronized Wnt-inhibited or CIN+ cancer cells with low doses of Taxol
152 just before mitosis (Fig. 3D) was sufficient to restore abnormal microtubule growth rates and
153 suppressed chromosome missegregation (Fig. 3E,F) indicating that the abnormal microtubule
154 growth rates originate in S phase, and they are maintained until mitosis as a "cytoskeletal memory",
155 which ultimately causes missegregation of chromosomes during mitosis.

156

157 ***Replication stress does not link Wnt signaling and chromosome missegregation***

158 Since Wnt inhibition acts specifically during S phase to regulate mitosis we wondered whether
159 Wnt10b signaling might be linked to DNA replication, which is the main process during S phase of
160 the cell cycle. In fact, it is well established that DNA replication stress is a frequent condition in
161 chromosomally unstable cancer cells and associated with broad genome instability (Gaillard et al,
162 2015, Zeman et al, 2014). Moreover, recent studies have highlighted that replication stress also
163 impacts mitosis and causes abnormal microtubule dynamics, thereby explaining the concomitant
164 presence of replication stress and high chromosome missegregation rates in chromosomally
165 unstable cancer cells (Bohly et al, 2019, Bohly et al, 2022, Burrell et al, 2013, Fragkos et al, 2017,
166 Liu et al, 2014, Wilhelm et al, 2020). In agreement with this, we found that induction of replication
167 stress in chromosomally stable HCT116 cells by treatment with low concentrations of aphidicolin, a

168 specific inhibitor of DNA polymerases and well-established inducer of replication stress (Bohly et al,
169 2019, Bohly et al, 2022, Ikegami et al, 1978, Minocherhomji et al, 2015), increased mitotic
170 microtubule growth rates and chromosome missegregation (Fig. 4A,B). *Vice versa*, increased
171 microtubule growth rates and chromosome missegregation endogenously present in CIN+ cancer
172 cells were suppressed upon nucleoside supplementation, an established mean to alleviate
173 replication stress (Bohly et al, 2019, Burrell et al, 2013, Wilhelm et al, 2014) (Fig. 4C,D). Thus,
174 replication stress during S phase mimics Wnt inhibition with respect to the induction of mitotic errors
175 raising the question whether Wnt10b inhibition causes replication stress. To address this, we
176 employed DNA combing analysis, the gold standard method to measure the progression of individual
177 replication forks during DNA replication (Fig. 4E)(Moore et al, 2022). As expected, treatment with
178 aphidicolin reduced replication fork velocities (Fig. 4F). Similarly, CIN+ cancer cells exhibited slowed
179 fork progression indicating endogenous replication stress in chromosomally unstable cancer cells as
180 reported previously (Fig. 4F)(Bohly et al, 2019, Bohly et al, 2022, Burrell et al, 2013). However,
181 neither DKK1 treatment nor the loss of *EVI/WNTLESS* (HCT116-*EVI*/*WNTLESS* knock-out cells)
182 affected replication fork speed (Fig. 4F). Accordingly, no reduced inter-origin distances were found
183 upon Wnt inhibition (Fig. S3A), which is known to be a direct consequence of replication stress (Bohly
184 et al, 2022, Ibarra et al, 2008, Moiseeva et al, 2019). We also did not find a delay in S phase
185 progression, which would be otherwise expected in the presence of replication stress (Bartkova et
186 al, 2005, Gorgoulis et al, 2005) (Fig. S3C,D). Also, treatment of CIN+ cells with Wnt10b, which
187 rescued mitotic errors (Fig. 2F,G), did not affect replication stress in these cancer cells (Fig. 4F).
188 Together, inhibition of Wnt10b signaling affects mitotic chromosome segregation, but does not
189 directly impact on DNA replication dynamics in human cancer cells.

190

191

192

193 ***Wnt10b signaling acts downstream of replication stress to ensure faithful mitosis.***

194 Since Wnt inhibition does not impact on replication dynamics *per se*, we hypothesized that Wnt10b
195 signaling might act downstream of replication stress to ensure proper mitosis. This hypothesis was
196 supported by the rescue of mitotic errors in CIN+ cells, whose mitotic errors are triggered by
197 endogenous replication stress (Fig. 4C,D,F), after the activation Wnt10b signaling (Fig. 2 F,G). To
198 further address this, we induced replication stress during early S phase by pulse-treatment with
199 aphidicolin or hydroxyurea, which depletes cellular nucleotide pools (Fig. 5A)(Bianchi et al, 1986).
200 Both means of replication stress induction resulted in increased microtubule growth rates and
201 chromosome missegregation in the subsequent mitosis, both of which were suppressed by co-
202 treatment with Wnt10b, but not with Wnt3a (Fig 5B,C). Since replication stress-induced abnormal
203 microtubule growth rates may originate from S phase (Fig. 3) we also determined microtubule growth
204 rates during S phase upon induced replication stress (Fig. 5A) or using CIN+ cancer cells, which
205 suffer from endogenous replication stress (Fig. 4F). In fact, replication stress induced increased
206 microtubule growth rates already in S phase where they were suppressed by Wnt10b treatment (Fig.
207 5D). Together, our data indicate that Wnt10b signaling can act as a pathway during S phase that
208 suppresses mitotic errors induced by DNA replication stress in human cancer cells.

209

210 ***Wnt10b signaling suppresses replication stress-induced chromosome breaks.***

211 In addition to causing mitotic errors, replication stress is known to give rise to chromosomal breaks,
212 which form the basis of structural chromosome instability in cancer (Branzei et al, 2010, Zeman et
213 al, 2014). Since Wnt10b regulates mitotic errors in response to replication stress, we wondered if
214 Wnt10b signaling also affects the downstream generation of chromosomal breaks. To address this,
215 we induced replication stress with aphidicolin or hydroxyurea treatment during early S phase, either
216 in the presence or absence of Wnt10b or Wnt3a (Fig. 6A). As expected, we observed increased
217 chromosomal breakage upon replication stress as determined by chromosome spread analysis (Fig.

218 6B). Intriguingly, treatment with Wnt10b, but not with Wnt3a, significantly suppressed replication
219 stress-induced chromosomal breaks (Fig. 6C), indicating that Wnt10b indeed modulates the
220 generation of chromosomal breaks upon replications stress. Similarly, increased levels of
221 chromosomal breaks were also detectable in CIN+ cancer cells, which were suppressed upon
222 alleviation of replication stress upon nucleoside supplementation, indicating that these chromosomal
223 breaks resulted from endogenous replication stress present in these cancer cells (Fig. 6D).
224 Importantly, the replication stress-induced chromosomal breaks in these CIN+ cancer cells were
225 also efficiently suppressed upon Wnt10b, but not Wnt3a treatment (Fig. 6D). Further supporting the
226 role of Wnt10b signaling in suppressing chromosomal breaks downstream of replication stress, we
227 found that inhibition of Wnt signaling either upon DKK1 treatment or in *EVI/WNTLESS* knockout cells
228 induced Wnt10b-dependent chromosomal breaks as seen after replication stress (Fig. 6C). Taken
229 together, our results indicate that Wnt10b signaling functions as a rescue pathway downstream of
230 replication stress, preventing both mitotic chromosome missegregation as well as chromosome
231 breaks, two well-established consequences of DNA replication stress and hallmarks of genome
232 instability in human cancer.

233

234 **Discussion**

235 Our work revealed a yet unrecognized und unexpected function of Wnt10b signaling to protect cells
236 from mitotic errors and chromosomal breaks in response to DNA replication stress, which is a major
237 source for chromosomal instability (CIN) in human cancer (Igarashi et al, 2024, Zeman et al, 2014).
238 Thus, Wnt10b signaling might act as a suppressor of CIN that is a well-established driving force for
239 the generation of high genetic heterogeneity and variability in cancer supporting tumor evolution
240 towards aggressive growth phenotypes, metastasis and therapy resistance (Chen et al, 2025,
241 Sansregret et al, 2018).

242 Replication stress (RS) is a highly cancer-relevant condition that is characterized by slowed or stalled
243 DNA replication during S phase of the cell cycle. It can be triggered by various cellular conditions
244 including nucleotide shortage, the presence of abnormal chromosome structures, DNA damage or
245 activation of oncogenes such as *MYC, RAS* or *CYCLIN-E* and contributes to the induction of
246 structural chromosome aberrations that are frequently seen in cancer (Igarashi et al, 2024, Zeman
247 et al, 2014). In addition, recent work has uncovered that RS also affects mitosis by deregulating
248 mitotic microtubule dynamics and centrosome separation leading to chromosome missegregation,
249 thereby driving the evolvement of aneuploidy (Bohly et al, 2019, Bohly et al, 2022, Burrell et al, 2013,
250 Jaime-Soguero d et al, 2024, Wilhelm et al, 2019). With this, RS sits at the helm of CIN in cancer
251 cells.

252 Intriguingly, our work demonstrates that activation of Wnt10b signaling in cancer cells suffering from
253 RS is sufficient to suppress both, the generation of chromosomal breaks and of mitotic errors
254 indicating that Wnt10b acts to limit deleterious consequences of RS in cancer cells. In line with a
255 function of Wnt10b downstream of RS, we showed that Wnt10b signaling does not impact on DNA
256 replication dynamics in cancer cells *per se* and its inhibition neither causes slowed replication fork
257 progression nor activation of dormant origin firing, which is a cellular rescue mechanism to
258 compensate for slow replication and to ensure completion of DNA replication (Bohly et al, 2022,
259 Ibarra et al, 2008, Moiseeva et al, 2019). However, this stands in contrast to our recent findings in

260 pluripotent stem cells where Wnt3a signaling suppresses origin firing in S phase (Jaime-Soguero d
261 et al, 2024), which is also required for faithful mitotic chromosome missegregation (Bohly et al, 2022,
262 Jaime-Soguero d et al, 2024). It is note that pluripotent stem cells have high basal levels of replicative
263 stress and unique replication profiles (Kafer et al, 2022, Kurashima et al, 2024), which may contribute
264 to the difference on the Wnt involvement in replicative stress in comparision to cancer cells. Further
265 analysis on proteins that are regulated by Wnt3a and Wnt10b during S phase in stem cells and
266 somatic cells, respectively, are required to define the overlapping or non-overlapping pathways
267 involved in S phase and mitotic regulation in both cell systems.
268
269 Cancer cells typically exhibit mild RS, which is sufficient to trigger low levels of structural
270 chromosome aberrations and mitotic errors that are still compatible with cell survival and avoiding
271 cell cycle arrest. Severe RS, however, causes excessive stalling of replication forks often associated
272 with severe DNA damage, which reduces cell viability and causes cell cycle arrest via the activation
273 of replication checkpoint pathways (Zeman et al, 2014). These checkpoint mechanisms involving
274 kinases such as ATR and Chk1 fulfills protective functions to replication stressed cells by imposing
275 cell cycle halt and ensuring efficient re-start of fork progression upon repair and thereby, these
276 checkpoint functions are essential to cell viability (Simoneau et al, 2021). In contrast to checkpoint
277 activation, Wnt10b acts downstream of mild replication stress in the absence of checkpoint activation
278 either induced by very low concentrations of aphidicolin or endogenously present in chromosomally
279 unstable colorectal cancer cells (Bohly et al, 2019, Burrell et al, 2013). To avoid deleterious
280 consequences of RS, cancer cells evolved various adaptation mechanisms to cope with RS. For
281 instance, upregulation of proteins such as Timeless and Claspin is observed in cancer cells suffering
282 from replication stress and this alleviates slowed fork progression independently of the ATR-Chk1
283 checkpoint (Bianco et al, 2019). However, as shown by our DNA combing analysis, Wnt10b addition
284 does not improve replication fork velocities in cancer cells with mild RS indicating that Wnt10b does
285 not act directly on replication fork progression. Nevertheless, Wnt10b clearly has protective functions

286 in cells with RS and hence, upregulation of Wnt10b might be useful for cells suffering from RS. In
287 fact, in many cancer types Wnt10b is found to be upregulated, but it is currently unclear whether this
288 is associated with RS in these tumors (Perkins et al, 2023).
289 It is yet unknown how Wnt10b signaling suppresses mitotic errors and chromosomal breaks in
290 response to RS. It can be speculated that the alterations in microtubule dynamics seen upon Wnt10b
291 modulation are involved. Our work provides new evidence that abnormally increased microtubule
292 growth rates are an immediate response to RS readily during S phase and this alteration is
293 maintained until cells enter mitosis where it causes chromosome missegregation by affecting proper
294 spindle positioning as shown previously (Ertych et al, 2014). Thus, RS or Wnt inhibition triggers a
295 rapid increase of microtubule growth rates, which might have a yet unknown physiological function
296 in S phase. Interestingly, recent reports have indicated that dynamic microtubules are involved in
297 nuclear DNA repair through regulation of chromatin mobility involving the microtubule-LINC (linker
298 of nucleoskeleton and cytoskeleton) complex (Lawrence et al, 2016, Lottersberger et al, 2015). Such
299 microtubule-involving repair mechanisms might be activated upon RS to prevent additional effects
300 during DNA replication, but further detailed investigations are needed to address this intriguing
301 possibility.
302 It is remarkable that specifically Wnt10b acts during S phase of the cell cycle although it has been
303 suggested to activate canonical Wnt signaling involving Frizzled receptors, LRP co-receptors,
304 GSK3β kinase and the well-characterized β-catenin destruction complex (Wend et al, 2012).
305 However, we found that Wnt3a is much more potent to activate β-catenin dependent Wnt signaling
306 while have no function in response to RS indicating a highly specialized and β-catenin independent
307 role of Wnt10b during S phase. In agreement, we previously demonstrated that LRP and GSK3β-
308 dependent, but β-catenin-independent Wnt/STOP (Wnt mediated stabilization of proteins) signaling
309 regulates microtubule dynamics causing mitotic chromosome missegregation and aneuploidy
310 (Acebron et al, 2014, Acebron et al, 2016, Huang et al, 2015, Stolz et al, 2015a, Stolz et al, 2015b).
311 Based on this, we suggest that Wnt10b-activated signaling, although employing the same Wnt

312 pathway components, specifically regulates target proteins, possibly through Wnt/STOP, during S
313 phase to contribute to its function upon RS.
314 Overall, our work highlights Wnt10b signaling as an extracellular signaling pathway regulating
315 consequences of DNA replication stress and mitotic errors in human cancer cells. In the same line,
316 we recently reported similar roles for other extracellular signaling pathways such as BMP, WNT and
317 FGF signaling in embryonic stem cells linking genome instability to cell fate (Jaime-Soguero d et al,
318 2024) suggesting key roles for extracellular cues in the maintenance of genome stability.
319
320

Materials and Methods

Cell culture

HCT116 (RRID:CVCL_0291), SW480 (RRID:CVCL_054), SW620 (RRID:CVCL_0547) and HEK293T (RRID:CVCL_0063) cells were purchased from ATCC (Manassas, USA) and cultured in RPM1-1640 or DMEM medium (PAN Biotech, Germany). HCT116-*EVI/WNTLESS* knock-out cells were described previously (Augustin et al, 2017, Lin et al, 2021). Media were supplemented with 10% FBS (#AC-AB-0024, Anprotec, Germany) and 1% Penicillin/streptomycin (#AC-AB-0024, Anprotec, Germany) in a CO_2 incubator at 37°C with 5% CO2.

Generation of *WNT10B* knockout cells

HCT116-*WNT10B* knock-out cells were generated as previously described (Ran et al, 2013, Voloshanenko et al, 2017). A short-guide RNA for CRISPR/Cas9 (3'-GGAAGAATGCGGCTCTGACA-5') was designed using E-CRISP (http://www.e-crisp.org), purchased from Eurofins Inc. (Ebersberg, Germany) and cloned into a pSpCas9(BB)-2A-Puro (px459) plasmid, which was a gift from Feng Zhang (Addgene plasmid #48139; http://n2t.net/addgene:48139; RRID:Addgene_48139)(Ran et al, 2013). HCT116 cells were transfected and selected in culture medium containing 2 µg/ml of puromycin. Pools of cells were first expanded and a single cell clone was generated and further analyzed.

Cell treatments

Where indicated, cells were treated with 100 nM aphidicolin (sc-201535, Santa Cruz, USA) or 2 mM hydroxyurea (H8627-1G, Merck-Millipore, Burlington, UK) to induce replication stress. Replication stress was alleviated by treatment with additional nucleosides for 48 h (30 µM 2'-deoxyadenosine monohydrate (#sc-216290, Santa Cruz, USA), 30 µM 2'-deoxycitidine hydrochloride (#sc-220820, Santa Cruz, USA), 30 µM thymidine (#sc-296542, Santa Cruz, USA) and 30 µM 2'-deoxyguanosine

347 mono-hydrate (#sc-238433, Santa Cruz, USA) as described previously (Bohly et al, 2019, Wilhelm
348 et al, 2014). Cells were treated with 0.6 µM CHIR99021 (SML1046, Sigma Aldrich, Germany) to
349 inhibit GSK3β kinase. Increased microtubule growth rates were suppressed by treatment with 0.2 nM
350 Taxol (Paclitaxel, T7191-1MG, Sigma Aldrich, Germany) as shown previously (Ertych et al, 2014).
351 As controls cells were treated with H_2O or dimethyl sulfoxide (D1418, Sigma-Aldrich, Germany).
352 Cells were treated with 400 ng/ml of human recombinant Wnt3a (5036-WN/CF, R&D Systems,
353 Germany) or human recombinant Wnt10b (7196-WN/CF, R&D Systems, Germany) to induce ligand-
354 specific Wnt signaling, or with 600 ng/ml of human recombinant DKK1 (120-30-500, PeproTech,
355 Germany) to inhibit Wnt/LRP6 signaling. 0.1 % bovine serum albumine (8076.2, Carl Roth,
356 Germany) in PBS was used as control treatment for all recombinant proteins.
357
358 **Wnt reporter assay**
359 HEK293T cells were seeded in a 96-well dish and were transfected with 20 ng TCF firefly luciferase
360 (TOP-FLASH) plasmid and 2 ng CMV Renilla luciferase plasmid using ScreenFect® A according to
361 the manufacturer's protocol (ScreenFect GmbH, Germany). After 24 hours cells were treated with
362 purified Wnt ligands and incubated overnight. Cells were harvested in 1x Passive Lysis Buffer
363 (Promega, Germany) and processed according to the manufacturer's protocol. TOPFLASH
364 luciferase values were normalized to control Renilla luciferase values. Mean values (± SD) were
365 calculated from four independent experiments.
366
367 **Western blotting**
368 Secreted Wnt10b protein was detected by western blotting upon enrichment using Blue Sepharose
369 beads (17-0948-01, Th. Geyer Inc., Germany). Enriched Wnt10b was resolved on 10 % SDS PAGE
370 gels and detected by western blotting using anti-Wnt10b antibodies (MABN717, 1:1000, 5A7, Merck-
371 Millipore, Germany, RRID: AB_3675944). Anti-HSC70 antibodies (#sc- 7298, 1:1000, B-6, Santa
372 Cruz, USA, RRID: AB_627761) were used as loading control.

373

374 **Cell cycle analysis**

375 Cell cycle distribution and mitotic content was determined by FACS analysis using a BD
376 FACSCanto™ II (BD Biosciences, Germany) and analyzed using FACSDiva™ software (Version 6,
377 BD Biosciences), as described (Ertych et al, 2014).

378

379 **Measurements of microtubule plus-end growth rates**

380 To measure microtubule plus-end assembly rates, comets of fluorescently labelled microtubule end-
381 binding protein 3 (EB3) were tracked by live cell fluorescence microscopy. Cells were transfected
382 with pEGFP-EB3 (kindly provided by Linda Wordeman, USA) or pcDNA3-EB3- StayGold (kindly
383 provided by Atsushi Miyawaki, Japan) (Hirano M et al, 2022) plasmids and analyzed using a
384 DeltaVision Elite live cell microscope as previously described (Bohly et al, 2022, Ertych et al, 2014).
385 For mitotic measurements, cells were accumulated in mitosis by treatment with 2 µM
386 dimethylenastrone (#SML0905, Sigma-Aldrich, Germany). Average assembly rates were calculated
387 from 25 individual measurements per cell and a total of 30 cells from three independent experiments
388 were analyzed per condition.

389

390 **Cell synchronization**

391 To synchronize cells at the G1/S transition of the cell cycle, cells were synchronized by a double
392 thymidine block protocol as described (Schmidt et al, 2021). 2 mM thymidine (#sc-296542A, Santa
393 Cruz, USA) was added for 16 h. Cells were released into fresh culturing medium by washing with
394 fresh culturing medium every 5 min for 30 min, cultured for 8 h and subjected to a second thymidine
395 block for 16 h before releasing from the G1/S block. Cells were further analyzed at different time
396 points after the release.

397

398

399 **Treatment of cell cycle synchronized cells**

400 Cell cycle phase specific treatments (Fig. 2) were done using cells synchronized at the G1/S
401 transition using a double thymidine protocol. Cells were released for various times as indicated in
402 Fig. 2A and treated with DKK1, GSK3i, Wnt3a or Wnt10b for two hours followed by washout of the
403 reagents. Treatments specific to early S phase (Fig. 3) were achieved by release from G1/S
404 synchronization for two hours followed by washout of the treatments. Induction of replication stress
405 in early S phase (Fig. 5 and 6) was achieved in the same manner while treatment with hydroxyurea
406 was done two hours after the release from the G1/S block to avoid cell cycle arrest before cell enter
407 S phase. Hydroxyurea was washed out four hours later.

408

409 **Detection of chromosome missegregation**

410 The appearance of lagging chromosomes during anaphase was used as a measure for chromosome
411 missegregation as described previously (Cimini et al, 2001). Cells grown on glass cover slips were
412 enriched by cell cycle synchronization using a double thymidine block and release protocol
413 coverslips, fixed with 2 % p-formaldehyde/PBS for followed by treatment with ice-cold methanol at -
414 20°C for for 5 min. Mitotic spindles, kinetochores and chromosomes were detected by
415 immunofluorescence microscopy using anti-α-tubulin antibodies (1:700, sc-23948, Santa Cruz, USA;
416 RRID:AB_628410), anti-Cenp-C antibodies (1:1,000, PD030, MBL, USA; RRID:AB_10693556) and
417 Hoechst33342 (#H3570, Thermo Fisher Scientific, Germany; RRID:AB_3675235). Images were
418 captured using a Leica DMI6000B microscope (Leica, Germany) equipped with a Leica DFC360 FX
419 camera and Leica LAS-AF software (Leica, Germany). A lagging chromosome was defined as Cenp-
420 C-positive DNA clearly separated from the polar DNA masses in late anaphase cells.

421

422 **Detection of chromosomal breaks**

423 Chromosomal breaks were detected on metaphase chromosome spreads. Cells were treated with
424 2 μM dimethylenasteron for 3 h to enrich mitotic cells in prometaphase. Cells were harvested,

425 resuspended in 40 % (v/v) RPM1-1640 medium (PAN Biotech, Germany)/60% H_2O and fixed in
426 75 % methanol/25 % glacial acetic acid. Cells were suspended in 100% glacial acetic acid and
427 dropped onto pre-cooled microscopy slides. The slides were dried, and DNA was stained with
428 Giemsa solution (AppliChem, Darmstadt, Germany). Bright-field microscopy was performed using a
429 Leica DM IL LED microscope (Leica, Wetzlar, Germany) equipped with a ODC832 camera (Kern &
430 Sohn GmbH, Balingen-Frommern, Germany) to detect and to quantify the appearance of
431 chromosomes with visible breaks.
432
433 **Molecular DNA combing**
434 Molecular DNA combing was performed to determine DNA replication fork progression rates and
435 inter-origin distances as a measure for activation of additional origins (Moore et al, 2022). Newly
436 synthesized DNA was sequentially labelled with 100 µM 5-Chloro-2'-deoxyuridine (CldU; #C6891,
437 Sigma-Aldrich, Germany) and 100 µM 5-Iodo-2'-deoxyuridine (IdU; #I7125, Sigma-Aldrich,
438 Germany) for 30 min each. Cells were harvested and processed using the FiberPrep DNA extraction
439 kit (Genomic Vision, France) according to manufacturer's protocol. The isolated and purified ssDNA
440 was combed on salinized microscope slides (Genomic Vision, France) using a Molecular Combing
441 System (Genomic Vision, France). Combed DNA samples were stained with primary anti-CldU
442 antibodies (#ab6326, 1:10, BU1/75, ICR1, Abcam, UK, RRID:AB_305426), anti-IdU antibodies
443 (#347580, 1:10, B44, BD Biosciences, Germany, RRID:AB_10015219), anti-ssDNA antibodies
444 (#autoanti-ssDNA, 1:5, DSHB, USA, RRID:AB_10805144) and secondary antibodies conjugated to
445 Alexa Fluor 488 (A21121, 1:25, Invitrogen, Germany, RRID:AB_2535764), Alexa Fluor 594
446 (#150160, 1:25, Abcam, UK, RRID:AB_2756445), and BV421 (#563846, 1:25, BD Biosciences,
447 Germany, RRID:AB_2738449). Labelled DNA fibers were imaged using a Delta Vision Elite
448 microscope (Delta Vision, SA) equipped with a PCO edge sCMOS camera (PCO, USA) at 63x
449 magnification and labelled stretched of DNA were anlyzed to calculate fork speeds and inter-origin
450 distances as described (Bohly et al, 2022).

451

452 **Statistical analysis**

453 Statistical analysis was performed and graphs were drawn using GraphPad Prism 9.0 software
454 (GraphPad Software, USA). Mean values and standard deviations (SD) were calculated for each
455 experiment. Microtubule polymerization rate measurements and DNA combing analyses were
456 depicted as box plots, where the whiskers represent the 10th and 90th percentile, the boxes the 25th
457 and 75th percentile, the line in the boxes the median value and the plus sign within the boxes the
458 average value. All experimental results are based on at least three independently performed
459 biological replicates as indicated in the figure legends. Statistical analysis was performed using
460 unpaired two-tailed *t*-tests. The statistical analysis of the Wnt/β-Catenin signaling activity was
461 performed using and unpaired one-sample *t*-test using Microsoft Excel. Significances for
462 experiments are indicated as p-values: ns (not significant): $p \geq 0.05$, ∗: $p < 0.05$, ∗∗: $p < 0.01$, ∗∗∗: p
463 < 0.001.

464

465 **Data availability**

466 All raw data generated in this study will be made available. This study did not generate data that
467 were deposited in public databases.

468

469

470

Acknowledgments

We thank Atsushi Miyawaki, Feng Zhang and Linda Wordeman for providing plasmids. This work was funded by the Deutsche Forschungsgemeinschaft (DFG), project number 331351713 – SFB1324 (H. Bastians, G. Davidson, M. Boutros, S. Acebron). We acknowledge support by the Open Access Publication Funds of the Göttingen University.

Author Contributions

Experiments were carried out by A.H. and F.W., J.W. performed Wnt reporter assays and *WNT10B* knockout cells were generated by O.V.. Experiments were analyzed and interpreted by A.H., F.W. J.W., G.D., O.V., M.B., S.A. and H.B. H.B. supervised the research and S.A. co-supervised parts of the research. The manuscript was written by H.B. and A.H. and all authors discussed results and commented on the manuscript.

Conflict of interest

The authors declare no competing interests.

488 **References**

489 Acebron, P. S, Karaulanov, E., Berger, S. B, Huang, L. Y, Niehrs, C. (2014) Mitotic wnt signaling
490 promotes protein stabilization and regulates cell size. *Mol Cell* 54: 663-674.
491 Acebron, P. S, Niehrs, C. (2016) Beta-catenin-independent roles of wnt/lrp6 signaling. *Trends Cell*
492 *Biol* 26: 956-967.
493 Albrecht, V. L, Tejeda-Munoz, N., Robertis D, M. E (2021) Cell biology of canonical wnt signaling.
494 *Annu Rev Cell Dev Biol* 37: 369-389.
495 Augustin, I., Dewi, L. D, Hundshammer, J., Erdmann, G., Kerr, G., et al (2017) Autocrine wnt
496 regulates the survival and genomic stability of embryonic stem cells. *Sci Signal* 10:
497 eaah6829.
498 Bakhoum, F. S, Landau, A. D (2017) Chromosomal instability as a driver of tumor heterogeneity
499 and evolution. *Cold Spring Harb Perspect Med* 7: a029611.
500 Bartkova, J., Horejsi, Z., Koed, K., Kramer, A., Tort, F., et al (2005) DNA damage response as a
501 candidate anti-cancer barrier in early human tumorigenesis. *Nature* 434: 864-870.
502 Bastians, H. (2015) Causes of chromosomal instability. In *Recent results in cancer research*
503 *fortschritte der krebsforschung progres dans les recherches sur le cancer*, 200, 2015/09/18
504 edn, pp 95-113.
505 Bianchi, V., Pontis, E., Reichard, P. (1986) Changes of deoxyribonucleoside triphosphate pools
506 induced by hydroxyurea and their relation to DNA synthesis. *J Biol Chem* 261: 16037-
507 16042.
508 Bianco, N. J, Bergoglio, V., Lin, L. Y, Pillaire, J. M, Schmitz, L. A, et al (2019) Overexpression of
509 claspin and timeless protects cancer cells from replication stress in a checkpoint-
510 independent manner. *Nature communications* 10: 910.
511 Bohly, N., Kistner, M., Bastians, H. (2019) Mild replication stress causes aneuploidy by
512 deregulating microtubule dynamics in mitosis. *Cell Cycle* 18: 2770-2783.

513 Bohly, N., Schmidt, K. A, Zhang, X., Slusarenko, O. B, Hennecke, M., et al (2022) Increased
514 replication origin firing links replication stress to whole chromosomal instability in human
515 cancer. *Cell reports* 41: 111836.
516 Branzei, D., Foiani, M. (2010) Maintaining genome stability at the replication fork. *Nat Rev Mol Cell*
517 *Biol* 11: 208-219.
518 Burrell, A. R, Mcclelland, E. S, Endesfelder, D., Groth, P., Weller, C. M, et al (2013) Replication
519 stress links structural and numerical cancer chromosomal instability. *Nature* 494: 492-496.
520 Burrell RA, Mcclelland SE, Endesfelder D, Groth P, Weller MC, Shaikh N, Domingo E, Kanu N,
521 Dewhurst SM, Gronroos E, et al (2013) Replication stress links structural and numerical
522 cancer chromosomal instability. *Nature* 494: 492-496.
523 Cadigan, M. K, Waterman, L. M (2012) Tcf/lefs and wnt signaling in the nucleus. *Cold Spring Harb*
524 *Perspect Biol* 4:
525 Chen, X., Agustinus, S. A, Li, J., Dibona, M., Bakhoum, F. S (2025) Chromosomal instability as a
526 driver of cancer progression. *Nat Rev Genet* 26: 31-46.
527 Chen X, Agustinus AS, Li J, Dibona M, Bakhoum SF (2024) Chromosomal instability as a driver of
528 cancer progression. *Nat Rev Genet* 26: 31-46.
529 Cimini, D., Howell, B., Maddox, P., Khodjakov, A., Degrassi, F., et al (2001) Merotelic kinetochore
530 orientation is a major mechanism of aneuploidy in mitotic mammalian tissue cells. *J Cell*
531 *Biol* 153: 517-527.
532 Devillers, R., Santos D, A., Destombes, Q., Laplante, M., Elowe, S. (2024) Recent insights into the
533 causes and consequences of chromosome mis-segregation. *Oncogene* 43: 3139-3150.
534 Dwivedi, D., Harry, D., Meraldi, P. (2023) Mild replication stress causes premature centriole
535 disengagement via a sub-critical plk1 activity under the control of atr-chk1. *Nature*
536 *communications* 14: 6088.

537 Ertych, N., Stolz, A., Stenzinger, A., Weichert, W., Kaulfuss, S., et al (2014) Increased microtubule
538 assembly rates influence chromosomal instability in colorectal cancer cells. *Nat Cell Biol*
539 16: 779-791.
540 Ertych, N., Stolz, A., Valerius, O., Braus, H. G, Bastians, H. (2016) Chk2-brca1 tumor-suppressor
541 axis restrains oncogenic aurora-a kinase to ensure proper mitotic microtubule assembly.
542 *Proc Natl Acad Sci U S A* 113: 1817-1822.
543 Fragkos, M., Naim, V. (2017) Rescue from replication stress during mitosis. *Cell Cycle* 16: 613-
544 633.
545 Gaillard, H., Garcia-Muse, T., Aguilera, A. (2015) Replication stress and cancer. *Nat Rev Cancer*
546 15: 276-289.
547 Gorgoulis, G. V, Vassiliou, V. L, Karakaidos, P., Zacharatos, P., Kotsinas, A., et al (2005)
548 Activation of the DNA damage checkpoint and genomic instability in human precancerous
549 lesions. *Nature* 434: 907-913.
550 Hanahan D, Weinberg RA (2011) Hallmarks of cancer: The next generation. *Cell* 144: 646-674.
551 He, C. T, Sparks, B. A, Rago, C., Hermeking, H., Zawel, L., et al (1998) Identification of c-myc as a
552 target of the apc pathway. *Science* 281: 1509-1512.
553 Hinze, L., Pfirrmann, M., Karim, S., Degar, J., Mcguckin, C., et al (2019) Synthetic lethality of wnt
554 pathway activation and asparaginase in drug-resistant acute leukemias. *Cancer Cell* 35:
555 664-676 e667.
556 Hirano M, Ando R, Shimozono S, Sugiyama M, Takeda N, Kurokawa H, Deguchi R, Endo K, Haga
557 K, Takai-Todaka R, et al (2022) A highly photostable and bright green fluorescent protein.
558 *Nat Biotechnol* 40: 1132-1142.
559 Huang, L. Y, Anvarian, Z., Doderlein, G., Acebron, P. S, Niehrs, C. (2015) Maternal wnt/stop
560 signaling promotes cell division during early xenopus embryogenesis. *Proc Natl Acad Sci U*
561 *S A* 112: 5732-5737.

562 Ibarra, A., Schwob, E., Mendez, J. (2008) Excess mcm proteins protect human cells from
563 replicative stress by licensing backup origins of replication. *Proc Natl Acad Sci U S A* 105:
564 8956-8961.
565 Igarashi, T., Yano, K., Endo, S., Shiotani, B. (2024) Tolerance of oncogene-induced replication
566 stress: A fuel for genomic instability. *Cancers (Basel)* 16:
567 Ikegami, S., Taguchi, T., Ohashi, M., Oguro, M., Nagano, H., et al (1978) Aphidicolin prevents
568 mitotic cell division by interfering with the activity of DNA polymerase-alpha. *Nature* 275:
569 458-460.
570 Jaime-Soguero D, A., Hattemer, J., Bufe, A., Haas, A., Berg VD, J., et al (2024) Developmental
571 signals control chromosome segregation fidelity during pluripotency and neurogenesis by
572 modulating replicative stress. *Nature communications* 15: 7404.
573 Janssen, A., Burg VD, M., Szuhai, K., Kops, J. G, Medema, H. R (2011) Chromosome segregation
574 errors as a cause of DNA damage and structural chromosome aberrations. *Science* 333:
575 1895-1898.
576 Kafer, R. G, O'connor, Aisling, Rogers, Samuel, Osteil, Pierre, Nelson, B. C, et al (2022)
577 Replication stress tolerance and management differs between naïve and primed pluripotent
578 cells. *bioRxiv*: 2022.2005.2012.491744.
579 Kurashima, K., Kamikawa, Y., Tsubouchi, T. (2024) Embryonic stem cells maintain high origin
580 activity and slow forks to coordinate replication with cell cycle progression. *EMBO Rep* 25:
581 3757-3776.
582 Lawrence, S. K, Tapley, C. E, Cruz, E. V, Li, Q., Aung, K., et al (2016) Linc complexes promote
583 homologous recombination in part through inhibition of nonhomologous end joining. *J Cell*
584 *Biol* 215: 801-821.
585 Lin, C. Y, Haas, A., Bufe, A., Parbin, S., Hennecke, M., et al (2021) Wnt10b-gsk3beta-dependent
586 wnt/stop signaling prevents aneuploidy in human somatic cells. *Life Sci Alliance* 4:
587 e202000855.

588 Liu, Y., Nielsen, F. C, Yao, Q., Hickson, D. I (2014) The origins and processing of ultra fine
589 anaphase DNA bridges. *Curr Opin Genet Dev* 26: 1-5.
590 Lottersberger, F., Karssemeijer, A. R, Dimitrova, N., Lange D, T. (2015) 53bp1 and the linc
591 complex promote microtubule-dependent dsb mobility and DNA repair. *Cell* 163: 880-893.
592 Lukow, A. D, Sheltzer, M. J (2022) Chromosomal instability and aneuploidy as causes of cancer
593 drug resistance. *Trends Cancer* 8: 43-53.
594 Minocherhomji, S., Ying, S., Bjerregaard, A. V, Bursomanno, S., Aleliunaite, A., et al (2015)
595 Replication stress activates DNA repair synthesis in mitosis. *Nature* 528: 286-290.
596 Moiseeva, N. T, Bakkenist, J. C (2019) Dormant origin signaling during unperturbed replication.
597 *DNA Repair (Amst)* 81: 102655.
598 Moore, G., Sainz J, J., Jensen, B. R (2022) DNA fiber combing protocol using in-house reagents
599 and coverslips to analyze replication fork dynamics in mammalian cells. *STAR Protoc* 3:
600 101371.
601 Nusse, R., Clevers, H. (2017) Wnt/β-catenin signaling, disease, and emerging therapeutic
602 modalities. *Cell* 169: 985-999.
603 Paim, G. LM, Lopez-Jauregui, A. A, Mcalear, S. T, Bechstedt, S. (2024) The spindle protein ckap2
604 regulates microtubule dynamics and ensures faithful chromosome segregation. *Proc Natl*
605 *Acad Sci U S A* 121: e2318782121.
606 Perkins, S. R, Singh, R., Abell, N. A, Krum, A. S, Miranda-Carboni, A. G (2023) The role of wnt10b
607 in physiology and disease: A 10-year update. *Front Cell Dev Biol* 11: 1120365.
608 Ran, A. F, Hsu, D. P, Wright, J., Agarwala, V., Scott, A. D, et al (2013) Genome engineering using
609 the crispr-cas9 system. *Nat Protoc* 8: 2281-2308.
610 Sansregret, L., Vanhaesebroeck, B., Swanton, C. (2018) Determinants and clinical implications of
611 chromosomal instability in cancer. *Nature Reviews Clinical Oncology* 15: 139-150.

612 Schmidt, K. A, Pudelko, K., Boekenkamp, E. J, Berger, K., Kschischo, M., et al (2021) The p53/p73
613 - p21(cip1) tumor suppressor axis guards against chromosomal instability by restraining
614 cdk1 in human cancer cells. *Oncogene* 40: 436-451.
615 Schneikert, J., Behrens, J. (2007) The canonical wnt signalling pathway and its apc partner in
616 colon cancer development. *Gut* 56: 417-425.
617 Simoneau, A., Zou, L. (2021) An extending atr-chk1 circuitry: The replication stress response and
618 beyond. *Curr Opin Genet Dev* 71: 92-98.
619 Siri, O. S, Martino, J., Gottifredi, V. (2021) Structural chromosome instability: Types, origins,
620 consequences, and therapeutic opportunities. *Cancers (Basel)* 13: 3056.
621 Stolz, A., Bastians, H. (2015a) Fresh wnt into the regulation of mitosis. *Cell Cycle* 14: 2566-2570.
622 Stolz, A., Neufeld, K., Ertych, N., Bastians, H. (2015b) Wnt-mediated protein stabilization ensures
623 proper mitotic microtubule assembly and chromosome segregation. *EMBO Rep* 16: 490-
624 499.
625 Taelman, F. V, Dobrowolski, R., Plouhinec, L. J, Fuentealba, C. L, Vorwald, P. P, et al (2010) Wnt
626 signaling requires sequestration of glycogen synthase kinase 3 inside multivesicular
627 endosomes. *Cell* 143: 1136-1148.
628 Tamura, N., Shaikh, N., Muliaditan, D., Soliman, N. T, Mcguinness, R. J, et al (2020) Specific
629 mechanisms of chromosomal instability indicate therapeutic sensitivities in high-grade
630 serous ovarian carcinoma. *Cancer Res* 80: 4946-4959.
631 Tetsu, O., Mccormick, F. (1999) Beta-catenin regulates expression of cyclin d1 in colon carcinoma
632 cells. *Nature* 398: 422-426.
633 Tijhuis, E. A, Johnson, C. S, Mcclelland, E. S (2019) The emerging links between chromosomal
634 instability (cin), metastasis, inflammation and tumour immunity. *Molecular cytogenetics* 12:
635 17.
636 Voloshanenko, O., Gmach, P., Winter, J., Kranz, D., Boutros, M. (2017) Mapping of wnt-frizzled
637 interactions by multiplex crispr targeting of receptor gene families. *FASEB J* 31: 4832-4844.

638 Wend, P., Wend, K., Krum, A. S, Miranda-Carboni, A. G (2012) The role of wnt10b in physiology
639 and disease. *Acta Physiol (Oxf)* 204: 34-51.
640 Wilhelm, T., Magdalou, I., Barascu, A., Techer, H., Debatisse, M., et al (2014) Spontaneous slow
641 replication fork progression elicits mitosis alterations in homologous recombination-deficient
642 mammalian cells. *Proc Natl Acad Sci U S A* 111: 763-768.
643 Wilhelm, T., Olziersky, M. A, Harry, D., Sousa D, F., Vassal, H., et al (2019) Mild replication stress
644 causes chromosome mis-segregation via premature centriole disengagement. *Nature*
645 *communications* 10: 3585.
646 Wilhelm, T., Said, M., Naim, V. (2020) DNA replication stress and chromosomal instability:
647 Dangerous liaisons. *Genes (Basel)* 11: 642.
648 Zeman, K. M, Cimprich, A. K (2014) Causes and consequences of replication stress. *Nat Cell Biol*
649 16: 2-9.
650 Zhan, T., Rindtorff, N., Boutros, M. (2017) Wnt signaling in cancer. *Oncogene* 36: 1461-1473.

651

652 **Figures**

653

654 **Figure legends**

655

656 **Figure 1 - Wnt10b signaling is required for normal microtubule dynamics and faithful**
657 **chromosome segregation during mitosis.**

658 **(A)** Model depicting the relationship between the loss of Wnt signaling, increased mitotic microtubule
659 plus-end growth rates, chromosome missegregation and the induction of aneuploidy.
660 **(B)** Experimental outline for the measurement of microtubule plus-end growth rates.
661 **(C)** Measurements of mitotic microtubule growth rates in HCT116, HCT116-*EVI* and HCT116-
662 *WNT10B* knock-out cells after Wnt inhibition. As indicated, cells were treated with DMSO (Ctrl),
663 600 ng/ml DKK1, 0.6 μM GSK3 inhibitor (CHIR-99021), 0.2 nM Taxol or 400 ng/ml of recombinant
664 Wnt ligands. Measurements are based on analysis of 25 microtubules/cell (n = 30 cells from three
665 independent experiments, two-tailed *t*-test). **(D)** Example images of cells with and without mitotic
666 chromosome missegregation. Fixed cells were stained for spindle microtubules (α-tubulin),
667 kinetochores (Cenp-C and chromosomes (DNA) to detect lagging chromatids during anaphase of
668 mitosis, scale bar 10 μm. **(E)** Quantification of the proportion of cells exhibiting chromosome
669 missegregation upon Wnt inhibition. Cells were treated as described in (C) and anaphase cells with
670 lagging chromosomes were quantified. Graphs show mean values ± SD (n = 300 cells from three
671 independent experiments, two-tailed *t*-test).

672

673 **Figure 2 - Wnt10b acts during S phase to promote faithful mitosis.**

674 **(A)** Schematic outlining cell cycle specific Wnt modulation using cell cycle synchronized cells
675 followed by analysis of mitotic outcomes. **(B)** Measurements of microtubule growth rates in HCT116
676 cells after cell cycle phase-specific treatment with 600 ng/ml DKK1 in the absence or presence of
677 0.6 μM GSK3β kinase inhibitor (25 microtubules/cell, n = 30 cells from three independent

678 experiments, two-tailed *t*-test). **(C)** Quantification of anaphase cells showing chromosome
679 missegregation upon treatments as described in (B). Graph shows mean values ± SD (n = 300 cells
680 from three independent experiments, two-tailed *t*-test). **(D)** Measurements of microtubule growth
681 rates in HCT116-*EVI/WNTLESS* knock-out cells after cell cycle-specific treatment with 400 ng/ml of
682 recombinant Wnt ligands (25 microtubules/cell, n = 30 cells from three independent experiments,
683 two-tailed *t*-test). **(E)** Quantification of HCT116-*EVI/WNTLESS* knock-out cells showing
684 chromosome missegregation after treatments as described in (D) (mean ± SD, n = 300 cells from
685 three independent experiments, two-tailed *t*-test). **(F)** Measurements of microtubule growth rates in
686 chromosomally unstable (CIN+) SW480 and SW620 colorectal cancer cells with or without treatment
687 with 400 ng/ml Wnt ligands during early S phase for two hours (25 microtubules/cell, n = 30 cells
688 from three independent experiments, two-tailed *t*-test). **(G)** Quantification of CIN+ cancer cells
689 displaying chromosome missegregation with or without treatments as in (F) (mean ± SD, n = 300
690 cells from three independent experiments, two-tailed *t*-test).
691
692 **Figure 3 – Wnt inhibition causes increased microtubule growth rates from S phase until**
693 **mitosis**
694 **(A)** Experimental setup for the cell cycle-specific analysis of microtubule growth rates. **(B)** Cell cycle
695 stage dependent measurements of microtubule growth rates after inhibition of Wnt signaling in
696 HCT116 upon DKK1 treatment or in HCT116 *EVI/WNTLESS* knock-out cells (20 microtubules/cell,
697 n = 30 cells from three independent experiments). **(C)** Cell cycle stage dependent measurements of
698 microtubule growth rates in chromosomally unstable colorectal cancer cells (20 microtubules/cell, n
699 = 30 cells from three independent experiments). **(D)** Experimental setup for the analysis of mitotic
700 microtubule assembly rates upon 0.2 nM Taxol treatment. **(E)** Measurements of mitotic microtubule
701 growth rates in the indicated cells with or without Taxol treatment at G2/M (20 microtubules/cell, n =
702 30 cells from three independent experiments). **(F)** Quantification of cells showing chromosome

703 missegregation after treatment as in (E)(mean ± SD, n = 300 cells from three independent
704 experiments, two-tailed *t*-test).
705

706 **Figure 4 - Replication stress does not link Wnt signaling and chromosome missegregation**

707 **(A)** Measurement of microtubule polymerization rates in HCT116 cells after induction of replication
708 stress. Cells were treated with 100 nM aphidicolin for 16 hours prior to live cell measurements of
709 microtubule growth rates (25 microtubules/cell, n = 30 cells from three independent experiments,
710 two-tailed *t*-test). **(B)** Quantification of anaphase cells showing chromosome missegregation upon
711 replication stress. HCT116 cells were treated as in (A) and chromosome missegregation was
712 detected in anaphase cells (mean ± SD, n = 300 cells from three independent experiments, two-
713 tailed *t*-test). **(C)** Measurement of mitotic microtubule growth rates in CIN+ cancer cells upon
714 alleviation of replication stress by nucleoside supplementation (25 microtubules/cell, n = 30 cells
715 from three independent experiments, two-tailed *t*-test). **(D)** Quantification of anaphase cells showing
716 chromosome missegregation upon treatment as in (C) (mean ± SD, n = 300 cells from three
717 independent experiments, two-tailed *t*-test). **(E)** Schematic setup for DNA combing to determine
718 replication fork speed and inter-origin distances. Representative examples of labelled unidirectional
719 DNA fibers are shown. **(F)** Determination of replication fork progression rates using the indicated
720 cells and treatments (>300 fibers per condition, n=1, two-tailed *t*-test).
721

722 **Figure 5 - Wnt10b signaling ensures faithful chromosome segregation after replication stress**

723 **(A)** Experimental outline for the analysis of mitotic errors after replication stress and Wnt treatment.
724 **(B)** Measurement of mitotic microtubule growth rates in HCT116 cells after treatment with 100 nM
725 aphidicolin (APH) or 2 mM hydroxyurea (HU) in the presence or absence of 400ng/ml Wnt ligands
726 (25 microtubules/cell, n = 30 cells from three independent experiments, two-tailed *t*-test) **(C)**
727 Quantification of anaphase cells showing chromosome missegregation after treatment as in (B)

728 (mean ± SD, n = 300 cells from three independent experiments, two-tailed *t*-test). **(D)** Measurements
729 of microtubule growth rates in early S phase upon replication stress. HCT116, SW480 and SW620
730 cells were synchronized in early S phase, treated as indicated and microtubule growth rates were
731 analyzed during S phase (25 microtubules/cell, n = 30 cells from three independent experiments,
732 two-tailed *t*-test).

733

734 **Figure 6 – Wnt10b suppresses replication stress-induced chromosomal breaks**

735 **(A)** Setup for the analysis of chromosomal breaks. **(B)** Representative images of chromosome
736 spreads with or without replication stress-induced chromosomal breaks. Scale bar, 5 µm and 10 µm
737 as indicated. **(C)** Quantification of chromosome breaks after replication stress or Wnt inhibition.
738 Mitotic chromosome spreads were analyzed from cells after induction of replication stress (100 nM
739 APH or 2mM HU) or after Wnt inhibition (DKK1, *EVI/WNTLESS* knockout) in the presence or
740 absence of Wnt ligands. The graph shows the number of chromosomes with breaks per cell (mean
741 ± SD, n=150 chromosome spreads from 3 experiments; two-tailed *t*-test). **(D)** Quantification of
742 chromosome breaks in CIN+ cancer cells after treatment with Wnt ligands or upon nucleosite
743 supplementation. The graph shows the number of chromosomes with breaks per cell (mean ± SD,
744 n=150 chromosome spreads from 3 experiments; two-tailed *t*-test).

745

746

Figure 1

A

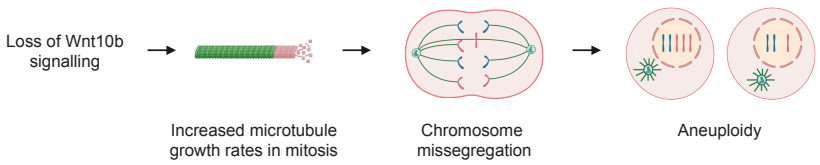

B

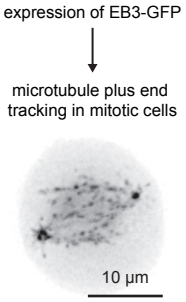

C

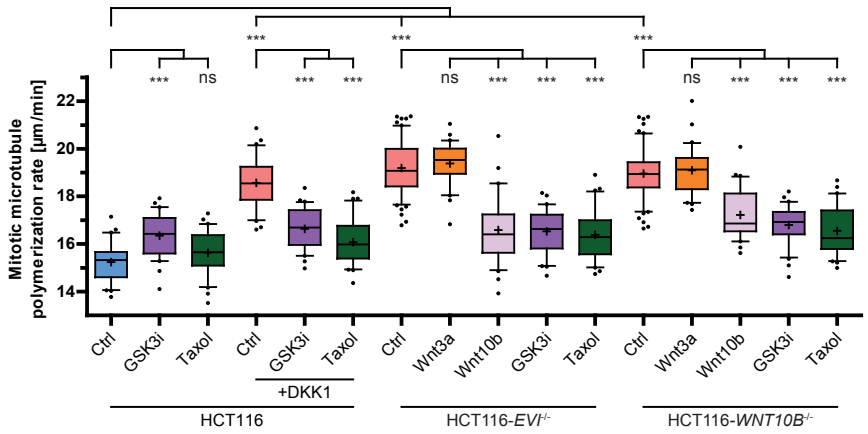

D

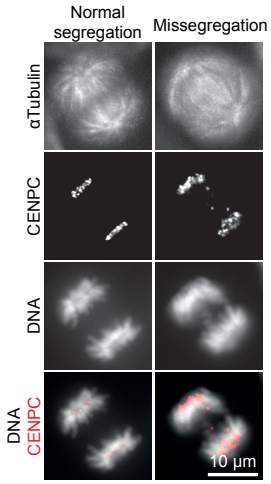

E

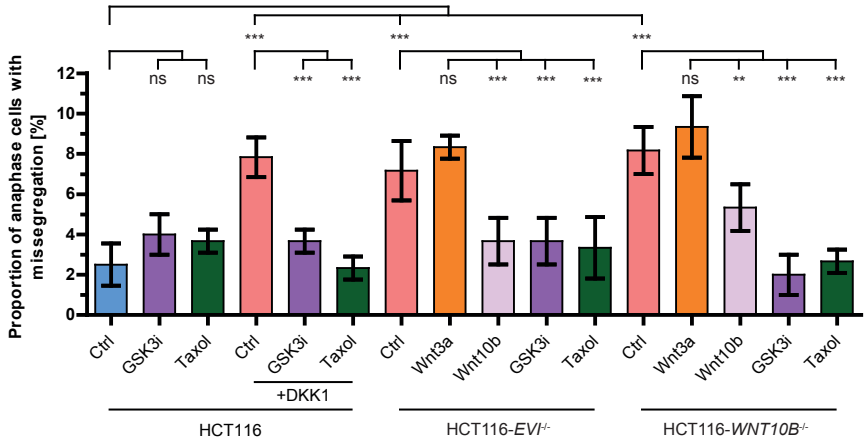

Figure 2

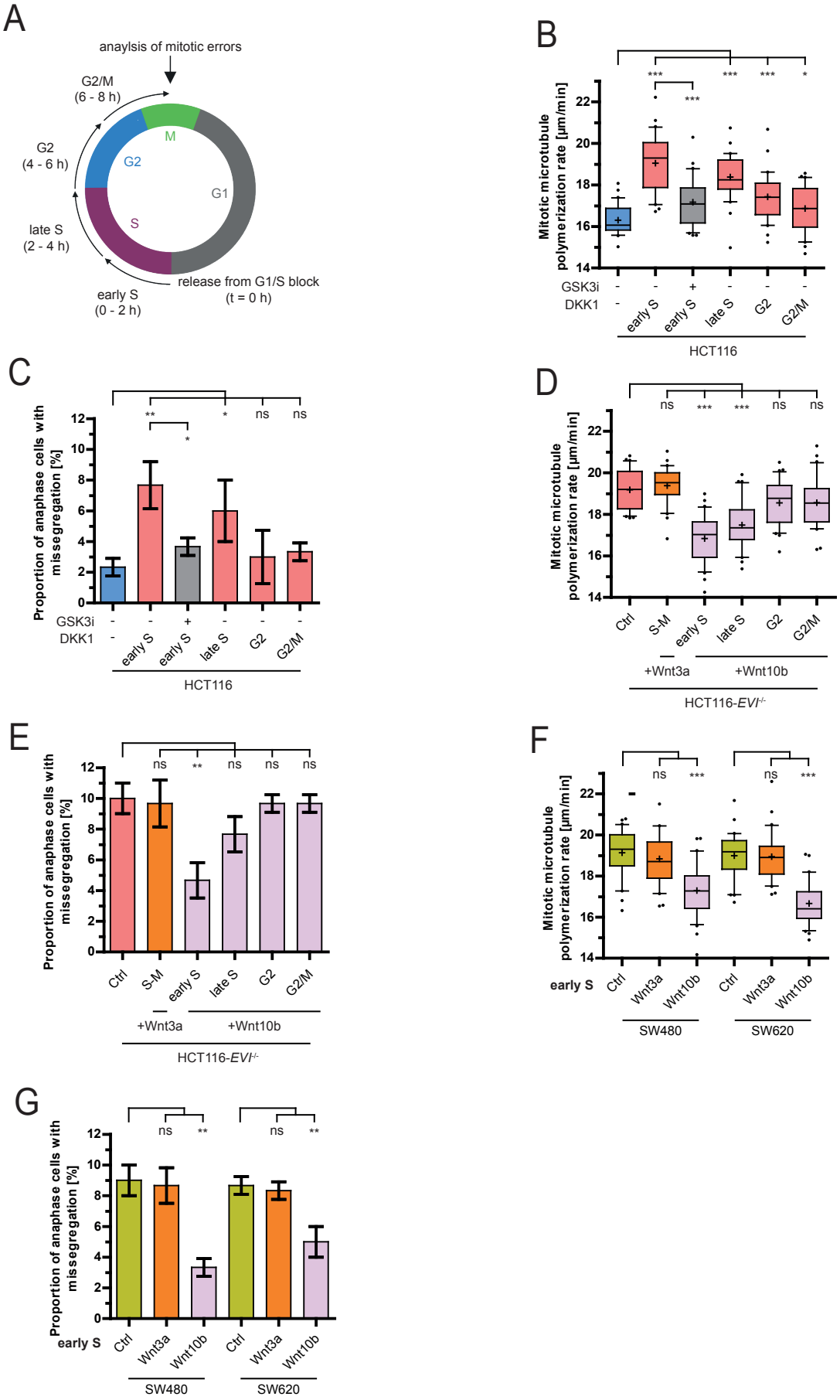
A
anaylsis of mitotic errors
G2/M
(6 - 8 h)
G2
(4 - 6 h)
late S
(2 - 4 h)
early S
(0 - 2 h)
M
G2
G1
S
release from G1/S block
(t = 0 h)
B
Mitotic microtubule polymerization rate [µm/min]
GSK3i
DKK1
early S
early S
late S
G2
G2/M
HCT116
C
Proportion of anaphase cells with missegregation [%]
GSK3i
DKK1
early S
early S
late S
G2
G2/M
HCT116
D
Mitotic microtubule polymerization rate [µm/min]
Ctrl
S-M
early S
late S
G2
G2/M
+Wnt3a
+Wnt10b
HCT116-EVI-/-
E
Proportion of anaphase cells with missegregation [%]
Ctrl
S-M
early S
late S
G2
G2/M
+Wnt3a
+Wnt10b
HCT116-EVI-/-
F
Mitotic microtubule polymerization rate [µm/min]
early S
Ctrl
Wnt3a
Wnt10b
Ctrl
Wnt3a
Wnt10b
SW480
SW620
G
Proportion of anaphase cells with missegregation [%]
early S
Ctrl
Wnt3a
Wnt10b
Ctrl
Wnt3a
Wnt10b
SW480
SW620

Figure 3

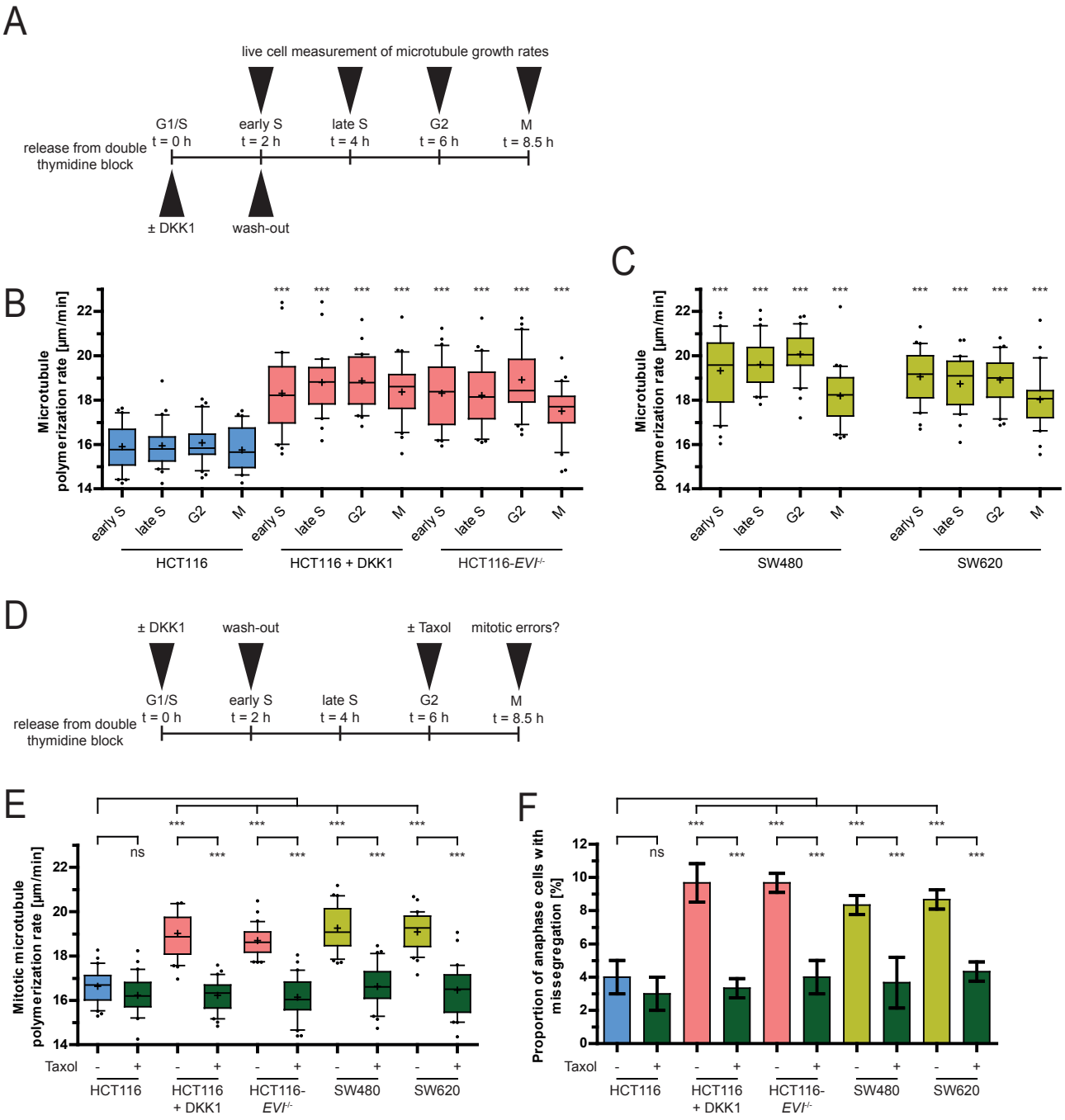
A
live cell measurement of microtubule growth rates
release from double thymidine block
G1/S t = 0 h
early S t = 2 h
late S t = 4 h
G2 t = 6 h
M t = 8.5 h
± DKK1
wash-out
B
Microtubule polymerization rate [µm/min]
early S
late S
G2
M
HCT116
HCT116 + DKK1
HCT116-EVI-/-
C
SW480
SW620
D
± DKK1
wash-out
± Taxol
mitotic errors?
E
Mitotic microtubule polymerization rate [µm/min]
ns
Taxol
HCT116
HCT116 + DKK1
HCT116-EVI-/-
SW480
SW620
F
Proportion of anaphase cells with missegregation [%]

Figure 4

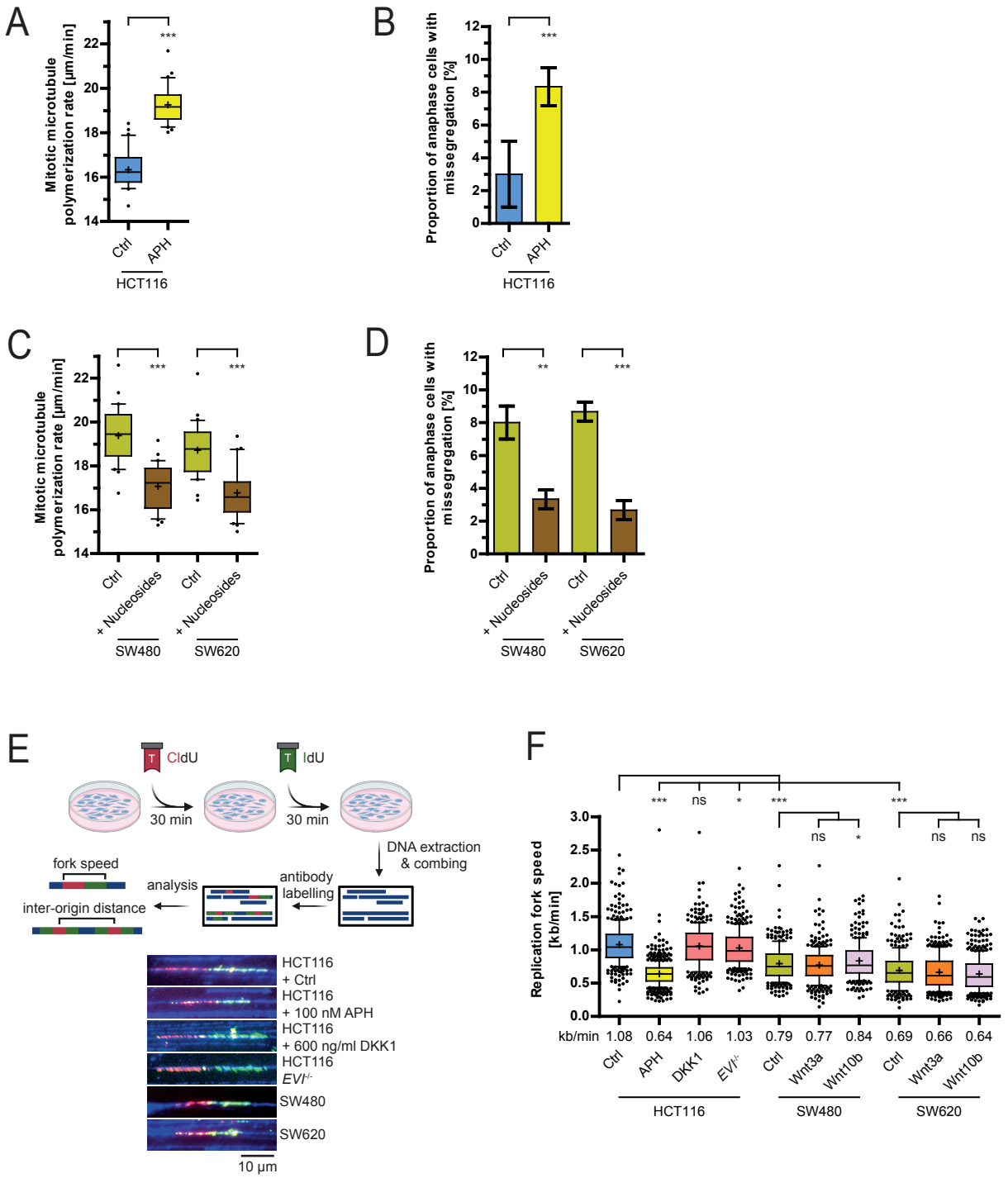
A
Mitotic microtubule polymerization rate [µm/min]
Ctrl
APH
HCT116
B
Proportion of anaphase cells with missegregation [%]
Ctrl
APH
HCT116
C
Mitotic microtubule polymerization rate [µm/min]
Ctrl
+ Nucleosides
Ctrl
+ Nucleosides
SW480
SW620
D
Proportion of anaphase cells with missegregation [%]
Ctrl
+ Nucleosides
Ctrl
+ Nucleosides
SW480
SW620
E
CldU
IdU
30 min
30 min
DNA extraction & combing
antibody labelling
analysis
fork speed
inter-origin distance
HCT116 + Ctrl
HCT116 + 100 nM APH
HCT116 + 600 ng/ml DKK1
HCT116 EVI-/-
SW480
SW620
10 µm
F
Replication fork speed [kb/min]
kb/min 1.08 0.64 1.06 1.03 0.79 0.77 0.84 0.69 0.66 0.64
Ctrl
APH
DKK1
EVI-/-
Ctrl
Wnt3a
Wnt10b
Ctrl
Wnt3a
Wnt10b
HCT116
SW480
SW620

Figure 5

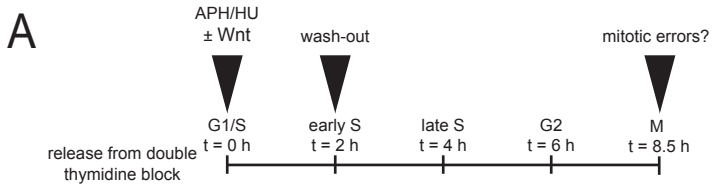
A
APH/HU
± Wnt
wash-out
mitotic errors?
release from double
thymidine block
G1/S
t = 0 h
early S
t = 2 h
late S
t = 4 h
G2
t = 6 h
M
t = 8.5 h

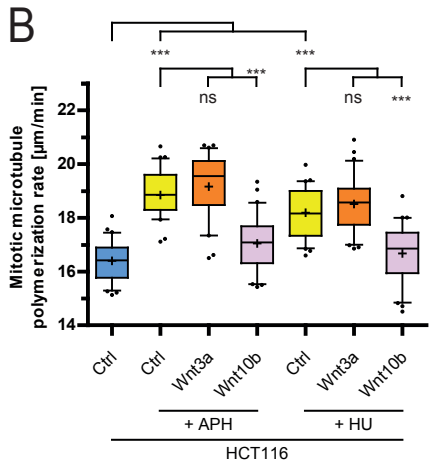
B
Mitotic microtubule
polymerization rate [µm/min]
Ctrl
Ctrl
Wnt3a
Wnt10b
Ctrl
Wnt3a
Wnt10b
+ APH
+ HU
HCT116
ns
ns
***

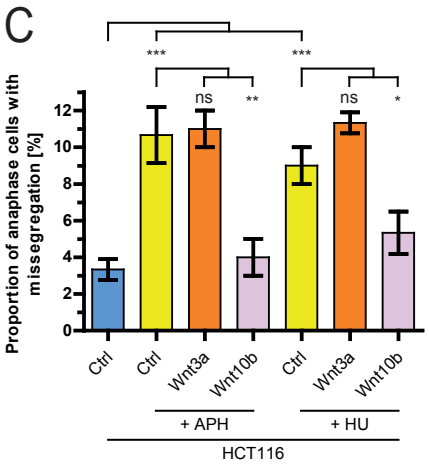
C
Proportion of anaphase cells with
missegregation [%]
Ctrl
Ctrl
Wnt3a
Wnt10b
Ctrl
Wnt3a
Wnt10b
+ APH
+ HU
HCT116
ns
ns
**
*
***

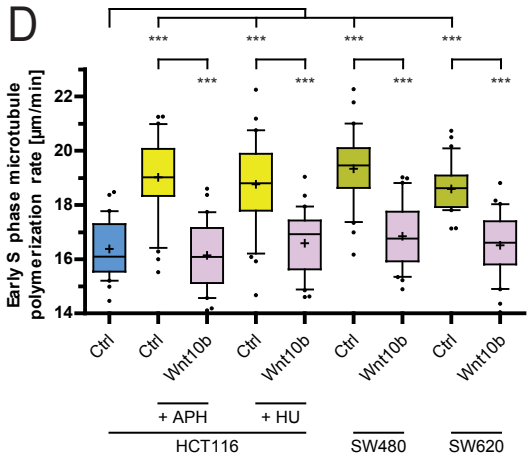
D
Early S phase microtubule
polymerization rate [µm/min]
Ctrl
Ctrl
Wnt10b
Ctrl
Wnt10b
Ctrl
Wnt10b
Ctrl
Wnt10b
+ APH
+ HU
HCT116
SW480
SW620
***

Figure 6

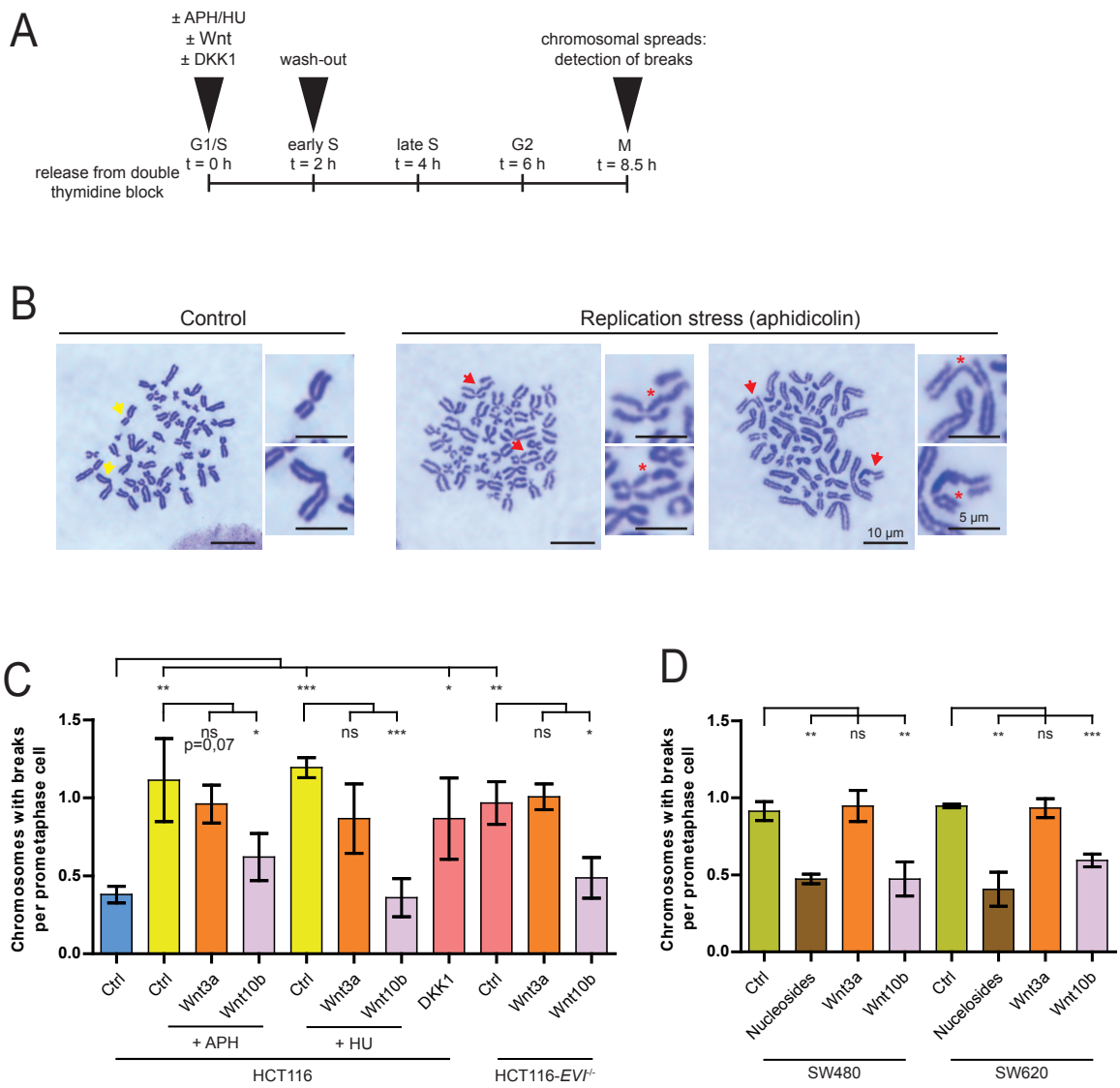
A
± APH/HU
± Wnt
± DKK1
wash-out
chromosomal spreads:
detection of breaks
G1/S
t = 0 h
early S
t = 2 h
late S
t = 4 h
G2
t = 6 h
M
t = 8.5 h
release from double
thymidine block
B
Control
Replication stress (aphidicolin)
10 µm
5 µm
C
Chromosomes with breaks
per prometaphase cell
1.5
1.0
0.5
0.0
ns
p=0,07
ns
ns
Ctrl
Ctrl
Wnt3a
Wnt10b
Ctrl
Wnt3a
Wnt10b
DKK1
Ctrl
Wnt3a
Wnt10b
+ APH
+ HU
HCT116
HCT116-EVI-/-
D
Chromosomes with breaks
per prometaphase cell
ns
ns
Ctrl
Nucleosides
Wnt3a
Wnt10b
Ctrl
Nucelosides
Wnt3a
Wnt10b
SW480
SW620